

# Comparative study of TL created in undoped CVD diamond by $\beta$ rays, UV and visible light

V. Chernov<sup>\*\*1</sup>, T. Piters<sup>1</sup>, P. W. May<sup>2</sup>, R. Meléndrez<sup>1</sup>, M. Pedroza-Montero<sup>1</sup>, and M. Barboza-Flores<sup>\*1</sup>

<sup>1</sup>Departamento de Investigación en Física de la Universidad de Sonora, Apartado Postal 5-088, Hermosillo, Sonora 83190, Mexico

<sup>2</sup>School of Chemistry, University of Bristol, Bristol, BS8 1TS, UK

Received 2 March 2010, revised 3 June 2010, accepted 8 June 2010

Published online 18 August 2010

**Keywords**  $\beta$  rays, CVD diamond, deconvolution, thermoluminescence, UV

\* Corresponding author: mbarboza@cajeme.cifus.uson.mx, Phone: +52 662 259 2156, Fax: +52 662 212 6649

\*\* e-mail chernov@cajeme.cifus.uson.mx

The thermoluminescence (TL) properties of CVD diamond film irradiated with  $\beta$  rays and illuminated with UV and visible light (200–450 nm) have been studied. The film (23  $\mu\text{m}$ ) was grown for 47 h on monocrystalline silicon. The TL glow curves are similar for  $\beta$  irradiation and short wavelength UV light. The  $\beta$  dose response curves and UV light time response curves exhibit linear–supralinear–sublinear behaviour. The structure of the glow curve was determined by a simultaneous deconvolution of a set of curves recorded after preliminary heating to various temperatures. One set of the TL peak parameters was found for

all the curves during the deconvolution. The TL glow curves were found to consist of five strongly overlapped peaks. The peaks at about 350 and 400 K obey first-order kinetics. The next three peaks at about 480, 540 and 580 K are described well by general-order kinetics. The TL curves created with light of wavelength between 250 and 450 nm are different from those created by  $\beta$  radiation and short wavelength UV light. The former have low sensitivity and consist of several strongly overlapped peaks, two of them are observed at about 330 and 600 K.

© 2010 WILEY-VCH Verlag GmbH & Co. KGaA, Weinheim

**1 Introduction** Chemical vapour deposition (CVD) synthetic diamond has been extensively studied for use as a radiation detector and thermoluminescence (TL) dosimeter mainly because of its unique properties that make it suitable for radiation dose measurements in biomedical applications. There are a number of publications in which the TL properties of undoped CVD diamond films are investigated. Most of these are devoted to TL created by ionizing radiation (see, for instance [1–3] and references therein). In several works [4–7] TL properties of films illuminated with light are also presented.

In this work we report the comparative analysis of TL glow curves of an undoped microcrystalline diamond film exposed to  $\beta$  rays and UV and visible light (200–450 nm).

**2 Experimental** The diamond film was grown for 47 h on monocrystalline silicon by the CVD method in a hot filament diamond reactor using 1%  $\text{CH}_4/\text{H}_2$  as precursor gases. The substrate was (100) oriented and had dimensions of about  $0.5 \times 5 \times 5 \text{ mm}^3$ . The thickness of the grown film

was 24  $\mu\text{m}$  and consisted of a polycrystalline layer with a columnar structure. It should be mentioned that the diamond film deposition process does not yet allow us to obtain standard TL properties that vary from sample to sample. In our case the TL properties were comparable to those measured previously by us on similar diamond films [8, 9].

All measurements and procedures on the substrate covered with the diamond film were performed inside an adapted Risø TL/OSL reader (model TL/OSL - DA-15). In this device, a cup with the sample was placed on a rotating table and automatically moved to several positions at which  $\beta$  irradiation (with a 33 mCi  $^{90}\text{Sr}$ - $^{90}\text{Y}$  source), light illumination and TL measurements were performed. TL curves were measured in the 330–630 nm range (Schott BG-39 filter) with the heating rate of 2 K/s. After each TL readout, the heater was disconnected from the cup to allow full cooling of the sample to RT, which required 300 s between TL readouts.

For UV and visible light illumination, the reader was coupled to a 300 W Oriel xenon arc lamp through an optical

© 2010 WILEY-VCH Verlag GmbH & Co. KGaA, Weinheim

fibre, an automated home-built shutter and a motorized Kratos, model GM252 monochromator. The bandwidth of the bleaching light was about 15 nm for entrance and exit slit values of 5 mm. The reader, the shutter and the monochromator were interfaced to a computer and controlled by a bespoke program. The computer program allowed subsequent experiments to be performed automatically. The fixed position of the sample in the cup guaranteed good reproducibility of the experiments.

The recorded TL glow curves were analysed with a homemade program, which allowed simultaneous deconvolution of several (up to eight) curves with one set of fitted parameters.

### 3 Results

**3.1 TL created with  $\beta$  rays** The TL glow curves and the TL dose response in the  $\beta$  dose range of 0.5–1000 Gy were obtained with a sequence of irradiations during 6–12 000 s, TL readouts from RT to 770 K and cooling to RT. The selected TL glow curves recorded immediately after  $\beta$  irradiation are depicted in Fig. 1. To fit on the same scale, the curves are normalized to delivered doses.

At low doses the glow curves exhibit unstructured TL between 320 and 640 K. With increasing dose the TL sensitivity (TL intensity divided by dose) increases (supralinearity). For doses higher than 100 Gy the TL intensity goes to saturation and is manifested in the decreasing of the sensitivity. The TL glow shape changes systematically indicating the presence of several strongly overlapped TL peaks with various degrees of supralinearity and saturation levels.

The TL dose responses at 350 and 540 K (averaged over 10 K intensities) corresponding to the two pronounced maxima on the high-dose curves are presented in Fig. 2. The dose response curves exhibit a typical linear–supralinear–sublinear behaviour that is observed for many thermoluminophors (the most known example is LiF:Mg,Ti [10]). It should be noted that irradiation with

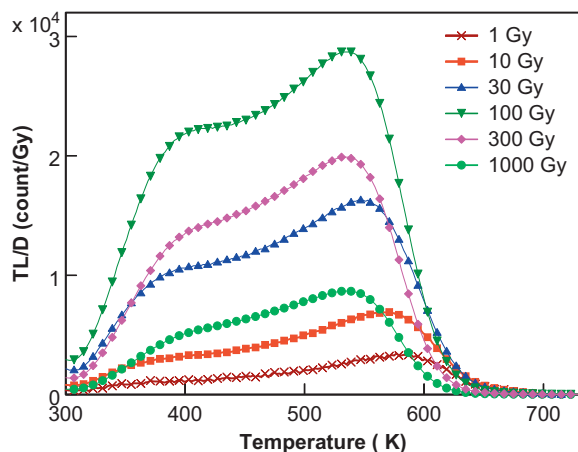


**Figure 1** (online colour at: www.pss-a.com) TL curves recorded after  $\beta$  irradiation with indicated doses (the curves are normalized to the dose values).

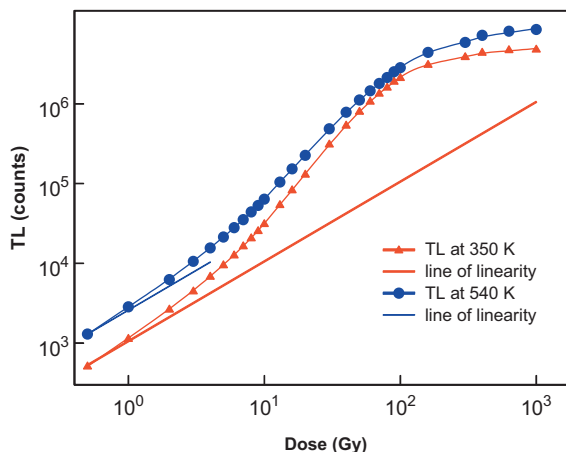


**Figure 2** (online colour at: www.pss-a.com) Growth of TL response, TL(D) at 350 and 540 K with  $\beta$  dose.

high doses followed by TL readout up to 770 K does not change the sensitivity of the sample.

**3.2 TL created with visible and UV light** The TL glow curves and the TL wavelength response in the case of light illumination were obtained with a sequence of illumination during 3600 s with wavelengths from 200 to 450 nm, step 10 nm, TL readouts from RT to 770 K and cooling to RT.

The selected TL glow curves recorded immediately after light illumination are depicted in Fig. 3. Because of the high variation of the intensity the curves are presented on a semilogarithmic scale. It is possible to divide the glow curve into two groups. The first group includes the curves created with short-wavelength light (200–260 nm). These curves exhibit sufficiently high TL intensity and look similar to the  $\beta$ -created curves. The second group of the curves created with longer wavelengths light have low sensitivity and consist of several strongly overlapped peaks. Two of these can be observed at about 330 and 600 K.

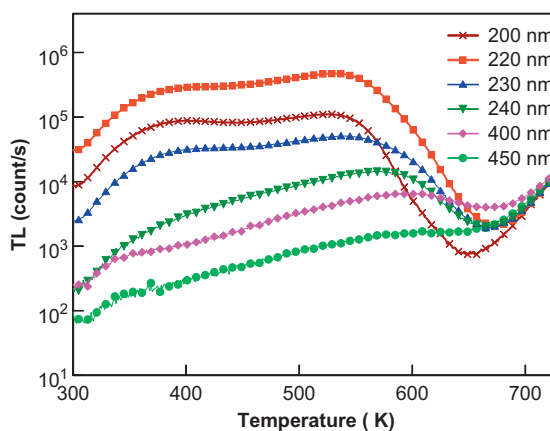


**Figure 3** (online colour at: www.pss-a.com) TL curves recorded after light illumination with indicated wavelengths during 1 h.

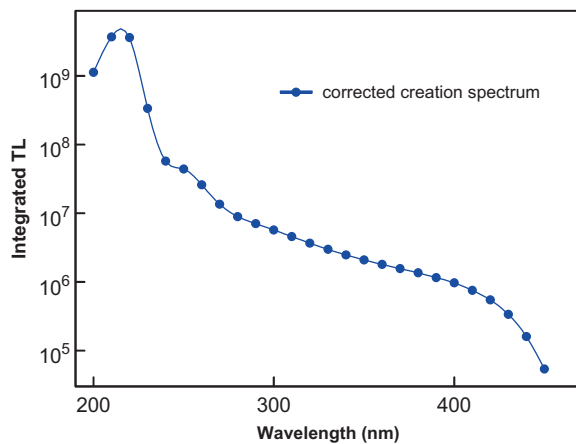


**Figure 4** (online colour at: [www.pss-a.com](http://www.pss-a.com)) Corrected creation spectrum of the integrated TL (from 310 to 670 K).

The dependence of TL response (taken as the integrated TL from 310 to 670 K) on the light wavelength is presented in Fig. 4. The intensity of the xenon lamp varies with the light wavelength. For this reason, the TL responses at each wavelength were normalized to the light intensity and the points in Fig. 4 represent the corrected creation spectrum of the integrated TL.

The creation spectrum consists of two parts. The first one is a band peaked at about 220 nm. The same band was found for natural (type IIb) diamond [11], CVD diamond films grown on silicon [12] and diamond [7] substrates. Its maximum position and an exponential increasing of the long-wavelength side indicate that the creation of TL in UV-irradiated CVD diamond is closely related to the fundamental absorption of UV light near the indirect band gap of diamond (5.45 eV, Ref. [13]). The spectrum between 250 and 450 nm is very broad and does not exhibit any features. A possible mechanism of the TL creation in this region can include the creation of free electrons due to light interaction

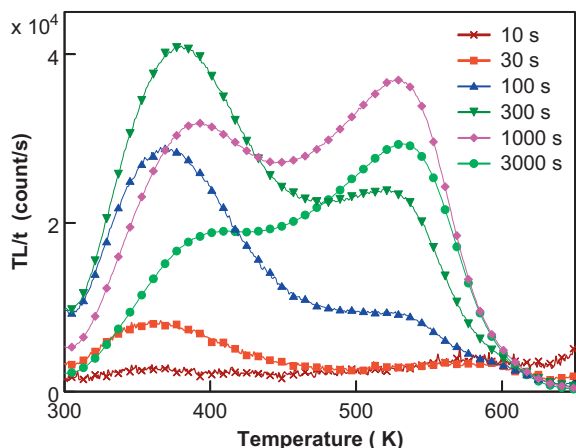


**Figure 5** (online colour at: [www.pss-a.com](http://www.pss-a.com)) TL curves recorded after 220 nm light illumination during indicated times (the curves are normalized to time values).

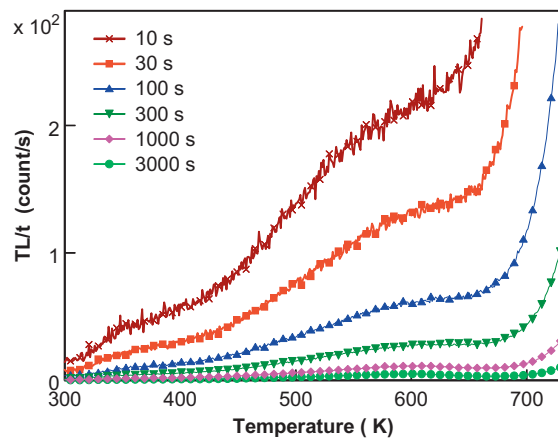


**Figure 6** (online colour at: [www.pss-a.com](http://www.pss-a.com)) TL curves recorded after 400 nm light illumination during indicated times (the curves are normalized to time values).

with the silicon substrate or the interlayer between the diamond film and the silicon.

The TL glow curves and the TL illumination time response were obtained with a sequence of illuminations during 10–3000 s with 220 and 400 nm light, TL readouts from RT to 770 K and cooling to RT. The TL glow curves recorded immediately after the illuminations are shown in Figs. 5 and 6. As in the case of the  $\beta$  irradiation, the curves are normalized to illumination time. The TL glow curves created by 220 nm light are similar to those of  $\beta$  irradiation. The only difference is the higher intensity of the low-temperature part of the curves relative to those at high temperatures (especially at low times). The TL created by 400 nm light consists of two broad peaks at about 360 and 600 K. The sensitivity of these peaks is low and decreases drastically with the increasing of illumination time.

The TL time responses at 350 and 540 K for 220 nm light are presented in Fig. 7. The 540 K curve is a linear–supralinear–linear behaviour (in the investigated time

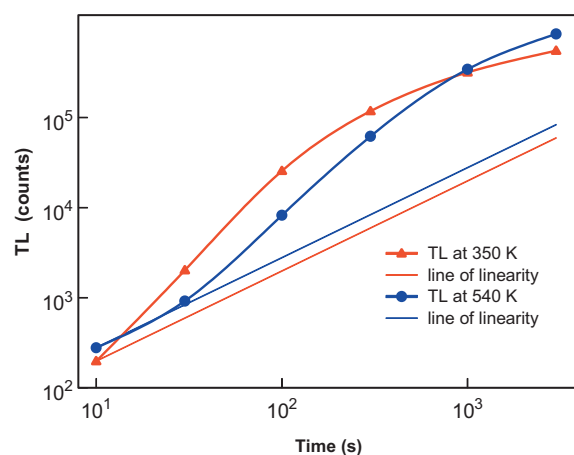


**Figure 7** (online colour at: [www.pss-a.com](http://www.pss-a.com)) Growth of TL response at 350 and 540 K with time for 220 nm light.

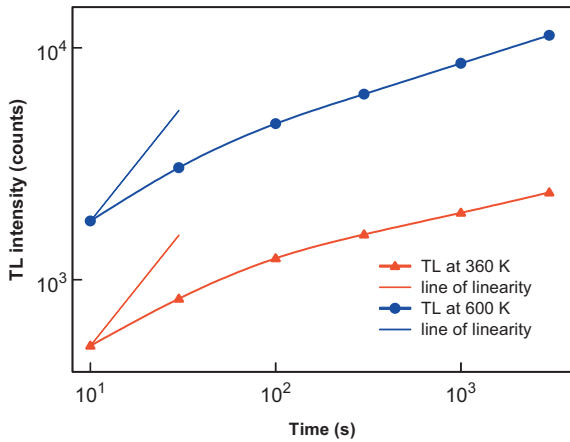


**Figure 8** (online colour at: www.pss-a.com) Growth of TL response at 360 and 600 K with time for 400 nm light.

interval) while the 390 K curve is supralinear–sublinear and does not exhibit a linear part. Figure 8 shows the TL time responses at 360 and 600 K for 400 nm light. Both curves are similar and exhibit sublinear behaviour.

**3.3 Deconvolution of TL curves** A deconvolution of TL glow curves into separate peaks is now a routine procedure. There are many publications in which deconvolution has been applied to analysis of CVD diamond TL. In the case of single or weakly overlapped peaks deconvolution is straightforward and gives reasonable results. In the opposite case, when the peaks are strongly overlapped and the number of the peaks is unknown, deconvolution is ambiguous. In fact, it is easy to obtain a good fit for any complex TL curve, but the result of the fitting will strongly depend on a subjective selection of the number of peaks and initial values of fitted parameters. This is because various combinations of the peak parameters can fit the TL curve with more or less equal precision.

It is possible to see from the figures presented above that the TL curves consist of several strongly overlapped peaks, but their number and positions are unclear. To clarify the structure of the glow curves a thermal cleaning procedure was carried out both for the  $\beta$  irradiation and the 220 nm light illumination. This procedure consists of the following repeated steps: 10 Gy  $\beta$  irradiation or 100 s 220 nm light illumination, preliminary TL readout up to a preheat temperature, cool down to RT, second TL readout up to 770 K (preheated glow curves), cool down to RT. The preheat temperature was changed from 320 to 670 K with step-size of 10 K. Figures 9 and 10 show the initial (recorded immediately after irradiation or illumination) and several preheated TL glow curves. The preheated glow curves show the typical subsequent disappearance of the TL peaks. The disappearance of the peaks is accompanied by the shifting of their maxima towards higher temperatures. But it is difficult to reach a definite conclusion because the simultaneous decay of several first-order kinetics peaks or the decay of a

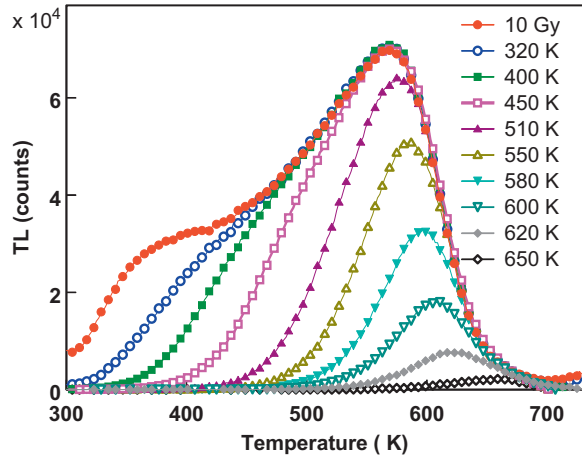


**Figure 9** (online colour at: www.pss-a.com) TL glow curves recorded immediately after  $\beta$  irradiation with 10 Gy and after preheats up to indicated temperatures.

single general-order kinetics peak. It is also unclear how many peaks the curves consist of.

To overcome this complicated situation and to carry out an appropriate deconvolution we applied a simultaneous fitting of parameters to a selected set of the glow curves obtained with the thermal cleaning procedure.

There are a number of models describing TL in irradiated solids. In this work, we will describe the TL peak shape  $I(T)$  with the general-order kinetics equations in the form proposed by Rasheedy [14]:

$$I(T) = -\eta \frac{dn}{dt} = \eta s \frac{n(T)^b}{N^{b-1}} \exp\left(-\frac{E}{kT}\right), \quad (1)$$

$$n(T) = \frac{n_0}{\left[1 + \frac{(b-1)s}{\beta} \left(\frac{n_0}{N}\right)^{(b-1)} \int_{T_0}^T \exp\left(-\frac{E}{kT_1}\right) dT_1\right]^{1/(b-1)}}, \quad (2)$$

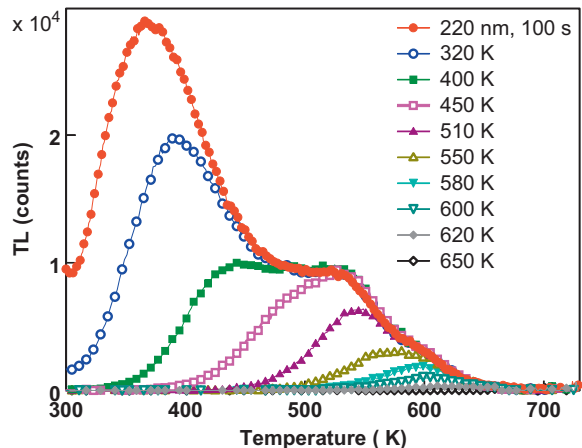


**Figure 10** (online colour at: www.pss-a.com) TL glow curves recorded immediately after 220 nm light illumination and after preheats up to indicated temperatures.

where  $n(T)$  and  $n_0$  are the current and initial concentrations of filled traps at temperatures  $T$  and  $T_0$ ,  $b$  is the kinetics order,  $E$  and  $s$  are the activation energy and frequency factor of the trap, respectively,  $k$  is the Boltzmann constant,  $N$  is a parameter related (equal in accordance with Rasheedy [14]) to the total concentration of the traps,  $\beta$  is the heating rate, and  $\eta$  is a constant relating the emptying rate for the filled traps with the measured TL intensity.

From the left part of Eq. (1) follows that

$$A(T) = \int_{T_0}^T I(T_1) dT_1 = \eta \beta n(T),$$

$$A_0 = \int_{T_0}^{\infty} I(T) dT = \eta \beta n_0, \quad (3)$$

where  $A_0$  is the total area of the TL peak.

Taking into account Eq. (3), we can rewrite Eq. (2) in the following way:

$$A(T) = \frac{A_0}{\left[ 1 + \frac{(b-1)s_1}{\beta} A_0^{b-1} \int_{T_0}^T \exp\left(-\frac{E}{kT_1}\right) dT_1 \right]^{1/(b-1)}}, \quad (4)$$

where the effective frequency factor

$$s_1 = s / (\eta \beta N)^{b-1}. \quad (5)$$

The Risø TL/OSL reader measures the TL sum-light per point:

$$I_{av}(T) = \frac{A(T + \Delta T) - A(T)}{\Delta T / \beta}, \quad (6)$$

where  $\Delta T$  is the increase in temperature per point during heating.

Equations (4)–(6) are the fitting expressions that we use in this work for describing the initial (without preliminary heating) TL glow curve. There are four fitting parameters:  $b$ ,  $E$ ,  $s_1$  and  $A_0$ . The preheated TL glow curves are described by the same expressions. The only difference is the reduction due to the preliminary heating of the initial TL peak area

$$A_p(T_p) = \frac{A_0}{\left[ 1 + \frac{(b-1)s_1}{\beta} A_0^{b-1} \int_{T_0}^{T_p + \Delta T_p} \exp\left(-\frac{E}{kT_1}\right) dT_1 \right]^{1/(b-1)}}. \quad (7)$$

Here an additional fitting parameter  $\Delta T_p$  was introduced to take into account a small reduction of the peak area caused by uncontrolled emptying of the traps during cooling after the preliminary heating.

Equations (4)–(7) represent the total set of the expressions that were used for the simultaneous fitting of the initial and  $N_c$  preheated glow curves. Each curve was

**Table 1** The kinetic parameters for the TL peaks created by (a)  $\beta$  irradiation with 10 Gy and (b) 220 nm light illuminated during 100 s.

| peak | maximum (K) <sup>a</sup> | kinetics order | activation energy (eV) | frequency factor <sup>b</sup> |
|------|--------------------------|----------------|------------------------|-------------------------------|
| 1a   | 355                      | 1.00           | 0.29                   | $7.4 \times 10^2$             |
| 2a   | 419                      | 1.00           | 0.33                   | $4.6 \times 10^2$             |
| 3a   | 495                      | 1.72           | 0.70                   | $4.5 \times 10^1$             |
| 4a   | 547                      | 1.50           | 0.92                   | $1.6 \times 10^4$             |
| 5a   | 588                      | 1.85           | 1.42                   | $3.7 \times 10^5$             |
| 1b   | 346                      | 1.00           | 0.30                   | $1.2 \times 10^3$             |
| 2b   | 391                      | 1.00           | 0.33                   | $8.1 \times 10^2$             |
| 3b   | 468                      | 1.35           | 0.64                   | $5.9 \times 10^3$             |
| 4b   | 525                      | 1.23           | 1.06                   | $7.8 \times 10^7$             |
| 5b   | 576                      | 1.60           | 1.24                   | $5.0 \times 10^6$             |

<sup>a</sup>For the non-first-order peaks the maximum shifts to higher temperatures with preheats; <sup>b</sup>The effective frequency factor has units of  $s^{b-2}/(\text{count}\cdot\text{K})^{b-1}$ .

supposed to consist of  $N_p$  overlapped peaks. The total number of the fitted parameters is equal to  $4 \times N_p + N_c \times N_p$ . The first term is the total number of peak parameters that are shared between all the curves, and the second term is the total number of parameters  $\Delta T_p$  which are individual for each peak of each preheated curve. It should be mentioned that Eqs. (4) and (7) are valid for  $b > 1$  only. So, for  $b < 1.01$  we used the standard equations for first-order kinetics.

The kinetics parameters of the TL peaks created with 10 Gy  $\beta$  irradiation are presented in Table 1 (peaks a). Simultaneous fitting was applied to the initial and seven preheated glow curves presented in Fig. 9. Two first-order kinetics and three general-order kinetics TL peaks were needed to obtain a good fit for the curves.

The quality of the fitting can be seen in Fig. 11 where the deconvolution of the initial glow curve is presented.

The deconvolution of the preheated curves is similar to those presented in Fig. 11. The only difference is the

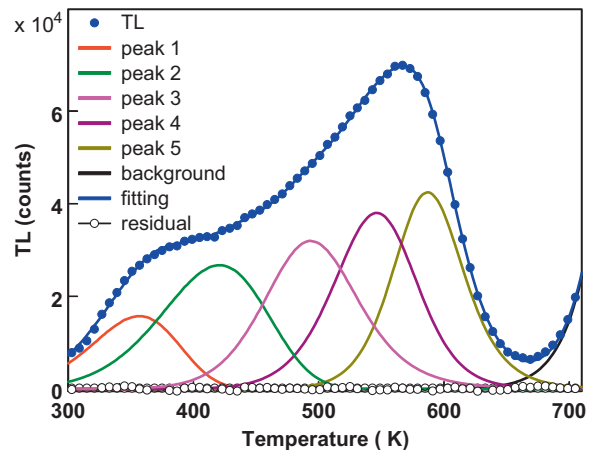


**Figure 11** (online colour at: www.pss-a.com) Deconvolution into separate peaks of the TL curve recorded immediately after  $\beta$  irradiation with 10 Gy.

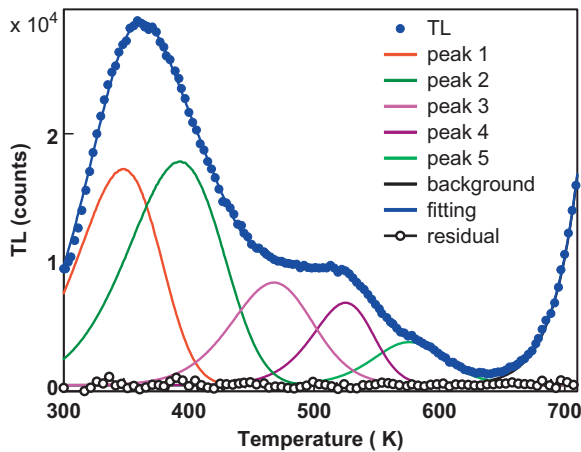


**Figure 12** (online colour at: [www.pss-a.com](http://www.pss-a.com)) Deconvolution into separate peaks of the TL curve recorded immediately after 220 nm light illumination.

systematic decay of the individual peaks (up to full disappearance) with increasing preheat temperature.

Table 1 (peaks b) presents the kinetics parameters of the TL peaks created with 220 nm light illumination that were obtained by the simultaneous fitting of the initial and seven preheated glow curves shown in Fig. 10. The deconvolution of the initial curve is shown in Fig. 12. As in the case of  $\beta$  irradiation, two first-order kinetics and three general-order kinetics TL peaks were needed to achieve good deconvolution results. The derived activation energies are also close to those derived from  $\beta$  irradiation.

**4 Conclusion** The TL glow curves created by  $\beta$  radiation, visible and UV light in the CVD diamond film grown on a silicon substrate were investigated. The TL properties are similar for  $\beta$  irradiation and short wavelength UV light illumination. The TL glow curves consist of five strongly overlapped peaks. The peaks at about 350 and 400 K obey first-order kinetics. The next three peaks at about 480, 540 and 580 K are described well by general-order kinetics. The dose response curves in the case of  $\beta$  irradiation and the time response curves in the case of UV light illumination exhibit linear–supralinear–sublinear behaviour.

The creation spectrum of UV illuminated CVD diamond film between 200 and 250 nm peaks at about 220 nm and exponentially decreases as the wavelength increases, and is closely related to the fundamental absorption of UV light near the indirect band gap of diamond. This suggests that the TL creation mechanisms for  $\beta$  radiation and short wavelength UV light illumination are similar. Both processes initiate the transition of electrons from the valence band to the conduction band. The electrons are then trapped by at least five different traps with activation energies from 0.3 to 1.4 eV. Electrons trapped by low-energy traps are emptied at RT and recombine with recombination centres causing the

afterglow observed immediately after irradiation or illumination [7, 8]. Heating from RT to high temperature empties each trap in turn creating TL peaks at temperatures about 350, 400, 480, 540 and 580 K.

The TL curves created with light between 250 and 450 nm are different from those created by  $\beta$  radiation and short wavelength UV light. The curves have low sensitivity and consist of several strongly overlapped peaks, two of which are observed at about 330 and 600 K. Their creation spectrum is very broad and does not exhibit any significant features. A possible mechanism for TL creation in this region may include the creation of free electrons due to light interaction with the silicon substrate or the interlayer between the diamond film and the silicon. To avoid a possible effect of the silicon substrate on TL properties it is preferable to carry out measurements on free-standing films. Because of the small thickness of these diamond films, this was not easy task, but we plan to do so in the near future.

**Acknowledgements** The financial support from CONACyT, (México) Grant Nos. 83536 and 82765, and SEP (México) is greatly acknowledged.

## References

- [1] J. Krása, B. Marczevska, V. Vorlíček, P. Olko, and L. Juha, *Diam. Relat. Mater.* **16**, 1510–1516 (2007).
- [2] M. Barboza-Flores, R. Meléndrez, V. Chernov, M. Pedroza-Montero, S. Gastelum, and E. Cruz-Zaragoza, *Mater. Res. Soc. Symp. Proc.* **1039**, 145–154 (2008).
- [3] R. Meléndrez, V. Chernov, P. W. May, B. Castañeda, M. Pedroza-Montero, and M. Barboza-Flores, *Phys. Status Solidi A* **206**, 2103 (2008).
- [4] L. M. Apátiga, V. M. Castaño, J. I. Goltzari, J. M. García, and F. Alba, *Mat. Res. Innovat.* **3**, 156 (1999).
- [5] B. Marczevska, C. Furetta, P. Bilski, and P. Olko, *Phys. Status Solidi A* **185**, 183 (2001).
- [6] A. Bizzarri, F. Bogani, M. Bruzzi, and S. Sciortino, *Nucl. Instrum. Methods A* **426**, 169 (1999).
- [7] M. Barboza-Flores, M. Schreck, S. Preciado-Flores, R. Meléndrez, M. Pedroza-Montero, and V. Chernov, *Phys. Status Solidi A* **204**, 3047–3052 (2007).
- [8] V. Chernov, T. M. Piters, R. Meléndrez, S. Preciado-Flores, P. W. May, and M. Barboza-Flores, *Phys. Status Solidi A* **206**, 2098–2102 (2009).
- [9] R. Meléndrez, V. Chernov, P. W. May, B. Castañeda, M. Pedroza-Montero, and M. Barboza-Flores, *Phys. Status Solidi A* **206**, 2103–2108 (2009).
- [10] J. Zimmerman, *J. Phys. C, Solid State Phys.* **4**, 3277 (1971).
- [11] N. Kristianpoller, D. Weiss, and R. Chen, *Physica B* **308–310**, 612, (2001).
- [12] M. Barboza-Flores, R. Meléndrez, V. Chernov, B. Castañeda, M. Pedroza-Montero, B. Gan, J. Ahn, Q. Zhang, and S. F. Yoon, *Radiat. Prot. Dosim.* **100**, 443 (2002).
- [13] O. Madelung, *Semiconductors: Data Handbook* (Springer, Berlin, 2004), p. 13.
- [14] M. S. Rasheedy, *J. Phys.: Condens. Matter* **5**, 633 (1993).